

## 2-3 Caesium Atomic Fountain Primary Frequency Standard NICT-CsF1

KUMAGAI Motohiro, ITO Hiroyuki, KAJITA Masatoshi, and HOSOKAWA Mizuhiko

NICT have developed Caesium atomic fountain primary frequency standard NICT-CsF1 to contribute to International Atomic Time (TAI) and Japan Standard Time. In NICT-CsF1, the caesium atoms are cooled and launched upward. Twice microwave interrogators give rise to the 1 Hz Ramsey resonance. All of the systematic shifts are evaluated with their uncertainty of  $1 \times 10^{-15}$ .

### *Keywords*

Caesium primary frequency standard, Atomic fountain, Ramsey resonance, Stability, Uncertainty

## 1 Introduction

### 1.1 Primary frequency standard

Atomic frequency standards are based on the idea of using the spectra generated by the discrete energy spacing of atoms, molecules or ions that remain permanent and invariable unless fundamental physical constants themselves change. Through experiments and verification using a variety of atomic species, the length of a second, which is a unit in the International System of Units (SI), was determined as follows at the 1967 General Conference of Weights and Measures;

“The second is the duration of 9192631770 periods of the radiation corresponding to the transition between the two hyperfine levels of the ground state of the caesium 133 atom.”

This definition is difficult to understand because it is written from the “time” point of view, however if this is changed to the “frequency” point of view, which is the inverse of time, it will become “the energy intervals between the hyperfine levels of the caesium atom are  $9192631770 \text{ Hz} (\times \text{Planck's Constant})$ ,” or “when a caesium atom is subjected to a 9192631770 Hz electromagnetic wave, the interior of the atom has the highest transition

probability to a different state”. So, if the frequency at which the caesium atom is most reactive (resonant frequency) deviates from 9192631770 Hz, then there must also be a deviation in the reference frequency. By using the International Atomic Time (TAI) and the Japan Standard Time (UTC (NICT)) as reference signals and observing the reaction of caesium atoms, it can be verified if the reference signal follows the definition of a second.

In addition, there are a number of definitions not covered in the above text. A more precise definition is as follows: the resonant frequency of a caesium atom is 9192631770 Hz under conditions that have absolutely no external perturbation; these include a temperature of zero Kelvin, zero external magnetic field and no external electric field, no collisions with other atoms or molecules, no gravitational effects, etc. However, because it is impossible to observe the signal under these conditions in an actual experiment, the value obtained from the caesium atoms is frequency shifted. Primary frequency standards are created so as to be able to evaluate all conceivable frequency shifts, and can realize the resonant frequency of a caesium atom in a condition with no perturbation. There are a variety of frequency standards in-

cluding commercial caesium clocks, hydrogen masers, rubidium atomic clocks, optical frequency standards. However these standards are at best secondary standards, and as of 2010 the only standard which can be truly called a primary frequency standard is the one that is based on the quantum transition of caesium atoms where all frequency shifts are evaluated.

The performance of primary frequency standards is evaluated based on two terms: “stability” and “uncertainty”. Stability expresses the reproducibility of the signal, and uncertainty expresses to what digit frequency shifts can be evaluated. For example, if the value can only be determined up to the 1Hz digit, 1Hz is smaller than 9192631770 Hz by ten digits, so it will have an uncertainty of  $10^{-10}$ . Similarly, an uncertainty of  $1 \times 10^{-15}$  is equivalent to evaluation of frequency shifts to  $10\mu\text{Hz}$  resolution. Primary frequency standards are built with priority on precision and are not generally suited to consecutive operation. For this reason, it is more accurate to refer to them as “calibration equipment” which is used periodically to check the values of the International Atomic Time and the Japan Standard Time than as “clocks” which are continually outputting a signal.

### 1.2 Ramsey resonance

In order to realize high precision primary frequency standards it is necessary to observe a resonance signal with the narrowest possible frequency linewidth. Due to quantum mechanics the longer the interaction time between atoms and the resonant microwave frequency probe, the narrower the resulting linewidth. However, it is not possible to maintain an atom motionless in the same location with no external perturbation, so it is impossible to observe a narrow line width signal using conventional techniques. The Ramsey resonance technique was devised to address this. Creating and widening a time interval between two successive interactions between atoms and the microwave field allows observation of a signal of the same linewidth as that of a continuous long interaction. Linewidth is the inverse of the interaction interval time (drift time), so the longer it is the

narrower the linewidth. The Ramsey resonance transition rate  $P(\tau)$  and linewidth  $\Delta\nu$  can be expressed as the following equation (see reference [1] for details).

$$P(\tau) = \frac{1}{2} \sin^2 b \tau [1 + \cos\{(\omega_0 - \omega)T\}] \quad (1)$$

$$b = \frac{\mu_B B}{\hbar} \quad (2)$$

$$\Delta\nu = \frac{1}{2T} \quad (3)$$

$\omega_0$  is the resonant frequency of the atom,  $\omega$  is the microwave frequency,  $\mu_B$  is Bohr magneton,  $B$  is the microwave magnetic flux density,  $\tau$  is the time when the atom passes through the cavity and  $T$  is the drift time.

### 1.3 Atomic fountain primary frequency standard

Firstly a magnetic separator type and then a photo-excitation type were developed as primary frequency standards using the Ramsey resonance technique. In these two types, the interaction cavities between the atoms and microwaves are spatially separated, and a long drift time is constructed by driving the atom horizontally using a thermal beam. The primary frequency standard NICT-O1 used photo-excitation wherein the atoms travelled between interaction cavities separated by 1.5m at a speed of 200m/sec. The drift time was several dozen milliseconds and the linewidth was approximately 100Hz. To enable an even longer drift time a proposal was made for a method where the atom is launched straight up and then drops freely as a result of gravity. If the cavity is installed on the atom’s trajectory it can interact twice; once when the atom is launched up and once when it descends again. However, if an atom is launched upwards using a thermal beam as in the above two types, the atom will ascend too far and diffusion will make it impossible to obtain the return signal. To deal with this, a method was adopted where laser light is used to reduce the atom’s speed. A long

drift time was created by collecting and precisely launching the atoms using laser radiation pressure. Under gravitational free fall a drift time of approximately 1 second can be achieved by launching the atoms several dozens of centimeters. The manner in which atoms are launched straight up and then falling due to gravity looks like a “fountain,” thus they are called “atomic fountains” in English and a “genshi-sen” in Japanese[2]-[8]. The development of this atomic fountain was realized together with the technology required for the controlling of the atoms using laser cooling.

#### 1.4 Development details

NICT has been developing caesium primary frequency standards to contribute to International Atomic Time (TAI) and to increase the precision of Japan Standard Time[9]. NICT carried out its own development on an atomic fountain as a successor to the primary frequency standard using magnetic separation CRL-CS1[10] and photo-excitation NICT-O1 (formerly the CRL-O1)[11]. Observation of a Ramsey signal was successfully carried out using a prototype system in 2002 (refer to the previous special issue)[12][13]. Certain results were able to be obtained using the prototype, however, NICT revised all of the required tech-

nology components including vacuum equipment, optical systems and control systems and developed a compact and high performance system aimed at realizing greater stability and a greater degree of accuracy. This system is named “NICT-CsF1”[14] and its design began in the spring of 2003. System construction was carried out at the same time that No.2 building was at completion and it has been operating since 2006. The system received international recognition as a primary frequency standard in 2007 and has been contributing to Coordinated Universal Time and the International Atomic time.

## 2 Atomic fountain primary frequency standard NICT-CsF1

NICT-CsF1 is operated in a room that is entirely enclosed in a single layer of magnetic shielding, attenuating the effect of the Earth’s magnetism to 1/10. The entire room is temperature controlled to  $25\pm 0.2^{\circ}\text{C}$ , and the floor is floating on air suspension that isolates it from seismic vibration.

### 2.1 NICT-CsF1 Structure

The physical package structure of NICT-CsF1 is shown in Fig. 1 (b). NICT-CsF1 has



**Fig.1 (a)** Caesium Atomic Fountain Primary Frequency Standard NICT-CsF1

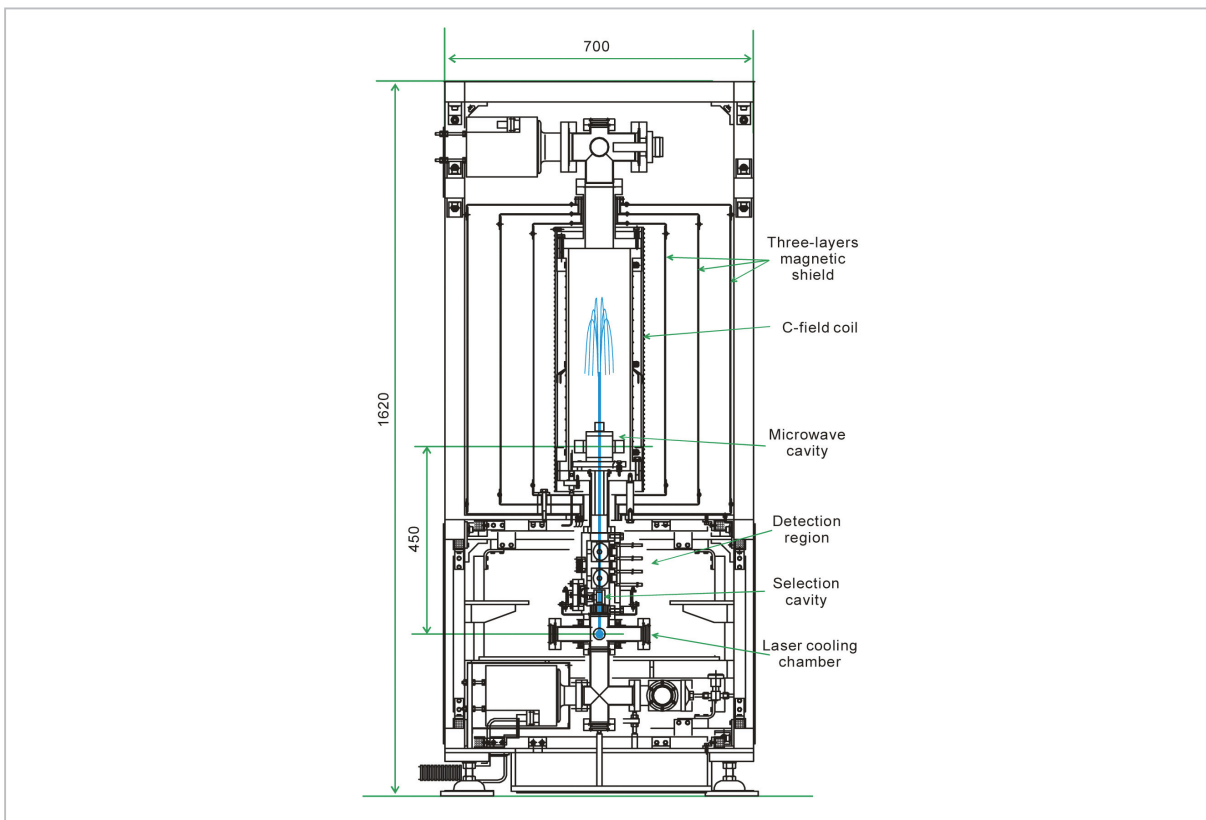


**Fig.1 (b)** Physical package structure of NICT-CsF1

three areas, a laser cooling area, a microwave interaction area, and a detection area. The detection area is located between the laser cooling area and microwave interaction area. The vacuum chamber (trap chamber) in the laser cooling area has view ports which allow input of multiple lasers so that atoms can be captured by laser light in all three dimensions. In addition, an anti-Helmholtz coil which generates a quadrupole magnetic field is attached to create a magneto-optical trap (MOT). The magnetic field gradient generated by the anti-Helmholtz coil is approximately 100mTesla/m. For laser cooling in NICT-CsF1 four horizontal lasers (XY plane) and two vertical lasers (Z axis) are used in an (0, 0, 1) arrangement. Compensation coils are wound around the aluminum frame which supports the trap chamber in all three axes: X, Y, and Z, and a small electric current is run through the coils to cancel the effect of the Earth's magnetic field. The cavity for selecting the  $m_F=0$  atoms (the clock transition) from the other atomic states is installed directly above

the laser cooling chamber (8cm above the trap chamber center). The selection cavity is a rectangular resonator using  $TE_{102}$  resonance mode with a Q value of approximately 100.

The microwave interaction area is composed of a cylindrical vacuum chamber (interaction chamber) and a three-layers magnetic shield. A C-field coil and cylindrical microwave cavity (Ramsey cavity) are installed inside the interaction chamber. The C-field coil is a cylindrical coil with a diameter of 20cm and a length of 60cm, and compensation coils are wrapped around the last 6cm of both ends to maintain the uniformity of the magnetic field. The resonant mode of the microwave cavity used to create the Ramsey resonance is  $TE_{011}$ , and the internal standing wave magnetic field is perpendicular to the C-field coil. The resonant cavity has a radius of 28mm and height of 23.3mm, and there are  $\phi 12$ mm holes in both the top and bottom end caps of the cavity to allow for the passage of the atoms. Microwave excitation to the cavity is carried out by micro-

wave probes attached to both sides. There are two degenerate modes,  $TM_{111}$  and  $TE_{011}$ . To suppress the unwanted  $TM_{111}$  mode a  $1/4$  wavelength choke structure is constructed inside the cavity. In addition, to prevent microwaves from escaping out of the holes for atom passage, 5cm long cut-off tubes are attached to the top and bottom end caps. In NICT-CsF1 the microwave cavity resonant frequency is adjusted so that it is as close as possible to the clock transition frequency (9.192631 GHz), with the difference maintained at 700kHz or less. The Q-value of the cavity itself is about 18,000, which is sufficiently low when compared to the atomic resonance Q-value (approx.  $10^{10}$ ), such that any frequency shift of the cavity can be ignored. The 3 layer magnetic shield around the interaction chamber is made of permalloy material and has a shielding ratio of approximately 1,000.

The detection area is composed of a rectangular vacuum chamber (detection chamber) and allows atoms to be illuminated by laser light from 3 positions at the top, bottom and center. In addition, there are view ports installed in 2 locations at the top and bottom in the direction where the laser light axes intersect, allowing for monitoring of the fluorescence emitted by the falling caesium atoms. The atoms emit fluorescence in all directions, so a spherical mirror is installed in the detection chamber to concentrate the light. After this the collected fluorescence is channeled through a light pipe and then onto a photo detector with a surface area of  $1\text{cm}^2$ . The center port is used during the photo-excitation which shifts the atoms from an  $F=3$  to  $F=4$  state. The detection method details are introduced in Section 3.1.

Carbon graphite tubes for absorbing excess caesium gas or microwave leaks are installed between the laser cooling area and detection area and between the detection area and microwave interaction area. The trap chamber and interaction chamber are each equipped with an ion pump and non-evaporable getter (NEG) pump which create a ultra-high vacuum of better than  $2 \times 10^{-7}$  Pa.

The total height of NICT-CsF1 structure is

approximately 1.6m, and the distance from the atom launch point to the microwave cavity is 45cm. The trap chamber and detection chamber are made of stainless steel (316L) which has a low magnetism, and the interaction chamber where the atoms interact with the microwaves is made of aluminum. The microwave cavity and fluorescence light gathering spherical mirrors are made of oxygen free copper. In addition, utmost caution is paid to ensure that no other magnetic bodies enter the vacuum layer.

## 2.2 Laser optical system

The optical setup of NICT-CsF1 is shown in Fig. 2. NICT-CsF1 uses 2 external cavity diode lasers as master lasers. The two lasers are frequency stabilized on the caesium atom  $D_2$   $F=4 \rightarrow F'=5$  line and the  $F=3 \rightarrow F'=2$  line. In

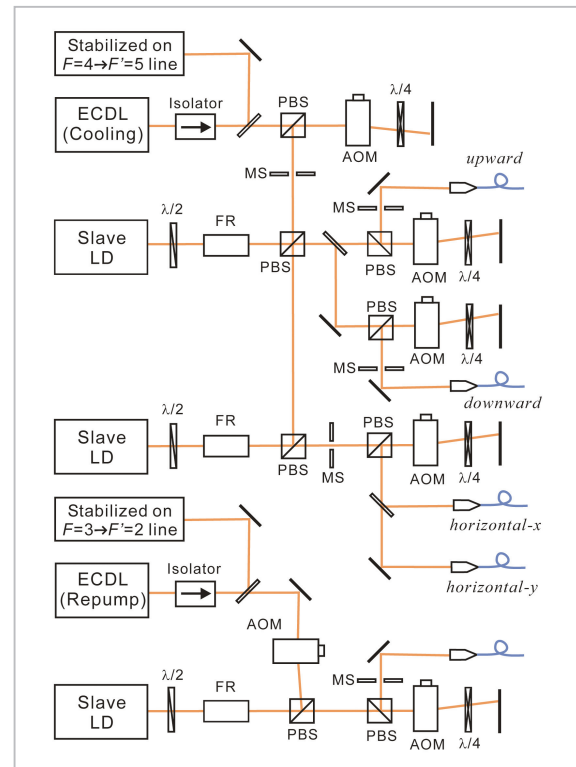


**Fig.2** Optical setup diagram for NICT-CsF1

ECDL: extended-cavity laser diode, FR: faraday rotator, PBS: polarizing beam splitter, AOM: acousto-optical modulator, MS: mechanical shutter. All laser beams are delivered to the chamber through polarization maintaining fibers.

order to increase long-term stability, the frequency stabilization error signal is obtained using the modulation transfer spectroscopy method<sup>[15]</sup>. The obtained frequency stability is  $10^{-12}$  even over long term measurements, in other words the laser frequency drift is maintained within a range of 1kHz.

In order to capture the largest number of atoms in laser cooling, the strength of the incident laser light must be sufficiently greater than the cooling transition saturation intensity. Because the master laser light strength is insufficient, the laser light is amplified by injection locking a 150mW single mode diode laser. NICT-CsF1 uses two 150mW lasers as slave lasers. The frequency and light strength of the amplified laser are controlled by an acousto-optic modulator (AOM). All of the AOM are driven by multichannel direct digital synthesizers (DDS), and switching of DDS frequency and strength is carried out within  $3\mu\text{s}$ . The turning ON/OFF of the laser light is carried at high speed by the AOM. In order to avoid so-called "light shift," any residual light not cut off by the AOM is completely blocked by mechanical shutters. In NICT-CsF1 five mechanical shutters are independently controlled. The optical table and main body of NICT-CsF1 are separated, and the laser light is conveyed to NICT-CsF1 by coupling the light into polarization maintaining fibers (PMF) using focusing lenses and quarter and half waveplates. At the output of the fibre the beams are collimated to a 25mm diameter (for horizontal beams) and 12mm (for vertical) that are circularly polarized. In addition a portion of the slave laser output is used for fluorescence detection. In the laser cooling and fluorescence detection processes, a repump light source for returning the  $F=3$  atoms to  $F=4$  is necessary, and one of the extended cavity laser diodes is used as this repump light source.

### 2.3 Microwave oscillator

A 9.192GHz highly stable and high resolution microwave synthesizer is required to probe the caesium atomic clock transition. At present a Spectra Dynamics Incorporation synthesizer (SDICS-1) is being used<sup>[16]</sup>. This synthesizer

is composed of a 5MHz voltage-controlled crystal oscillator (VCXO) and 100MHz VCXO, 9.2GHz dielectric resonant oscillator (DRO) and a 7.3MHz DDS, and the DDS is phase locked to a 5MHz external reference signal. For the external reference signal a hydrogen maser signal linked to UTC (NICT) is used. The oscillating frequency of the 9.192GHz synthesizer frequency can be altered at resolutions of  $1\mu\text{Hz}$  or less by PC controlling the synthesizer internal DDS. Spurious emissions and harmonic noise are 60dB or less for the carrier.

## 3 Atomic fountain standard operation

### 3.1 Operation cycle

The operation of NICT-CsF1 consists of a repetition of atom capture, launching upwards, polarization gradient cooling, state selection, Ramsey resonance (interaction with microwaves 2 times), detection, and capture of the atoms again. The MOT (400ms) captures approximately  $10^8$  caesium atoms, and cools them to the Doppler limit temperature (several hundred  $\mu\text{K}$ ). After the atoms are captured but before they are launched upwards the MOT coil current is turned off and the residual magnetic field dissipates for 40ms. In this time atoms maintained in their position are captured now solely by optical molasses (a syrup-like state where atoms concentrate at one point as a result of interaction between light and atoms). The cooled atoms are then launched upward using the 1 dimensional moving molasses technique (a technique where the downward oriented light frequency is shifted to a lower frequency and the upward oriented frequency is shifted to a higher frequency), providing the atoms with an initial upward velocity. In order to prevent saturation effects from the horizontal laser beams at this time, the horizontal beams are switched off at the initial stage of the launch (0.7ms). The horizontal lasers are then turned on again once the laser reaches its initial velocity to limit horizontal scattering of the atoms (0.3ms). The atoms, which have reached their maximal launch velocity, are then cooled

to approximately  $2\mu\text{K}$  via polarization gradient cooling (PGC). During this PGC stage the frequency of the laser light capturing the atoms is ramped away from the resonant frequency in steps ( $10\text{MHz}\rightarrow 50\text{MHz}$ ) while the laser strength is simultaneously weakened. By the time cooling via PGC is completed all of the laser light has been completely turned off by the AOMs and mechanical shutters.

When the launched atoms pass through the selection cavity, only the magnetic sublevel  $m_F=0$  atoms from among the  $F=4$  atoms are selectively excited to  $|F=3, m_F=0\rangle$ . The other remaining  $F=4$  sublevel atoms are blasted away by interacting with travelling laser light which resonates with  $F=4$  atoms, and only the  $|F=3, m_F=0\rangle$  atoms that remain continue to move upward. The  $F=3$  atoms pass through the Ramsey cavity on their way upward and interact with the microwaves. The atoms continue to move upwards while preserving the interaction information, then begin to fall again after reaching a height of approximately  $40\text{cm}$  above the cavity, then pass through the cavity again on their way down and react with the microwaves again. Ramsey resonance is triggered by this double interaction with the microwaves. Ramsey resonance excites the  $F=3$  atoms to an  $F=4$  state, however that excited state is dependent on the frequency of the microwaves fed into the cavity, and the frequency when the probability of excitement is highest will be  $9192631770\text{Hz}$  specified in the definition of a second.

As the number of atoms will fluctuate from launch to launch, it is necessary to normalize the signal. To do this a measurement of the total number of launched atoms is necessary, which requires an additional measurement of the number of atoms in the  $F=3$  state. Firstly, atoms in the  $F=4$  state are interrogated through the top port of the detection area and the fluorescence is observed, yielding  $N_4$ . After observing the fluorescence, the  $F=4$  atoms are subjected to a blasting laser traveling wave to remove them from the trajectory, leaving only the  $F=3$  state atoms. As these  $F=3$  atoms pass the middle port, repump laser light moves them

into the  $F=4$  state. The number of atoms is then determined by interrogating with detection laser light via the lower port of the detection area, yielding the number of atoms that had previously been in the  $F=3$  state,  $N_3$ . The ratio  $P=N_4/(N_4+N_3)$  yielding information of the number of atoms in each state and is not affected by fluctuation in the launched number of atoms.

In NICT-CsF1 atoms are launched with an

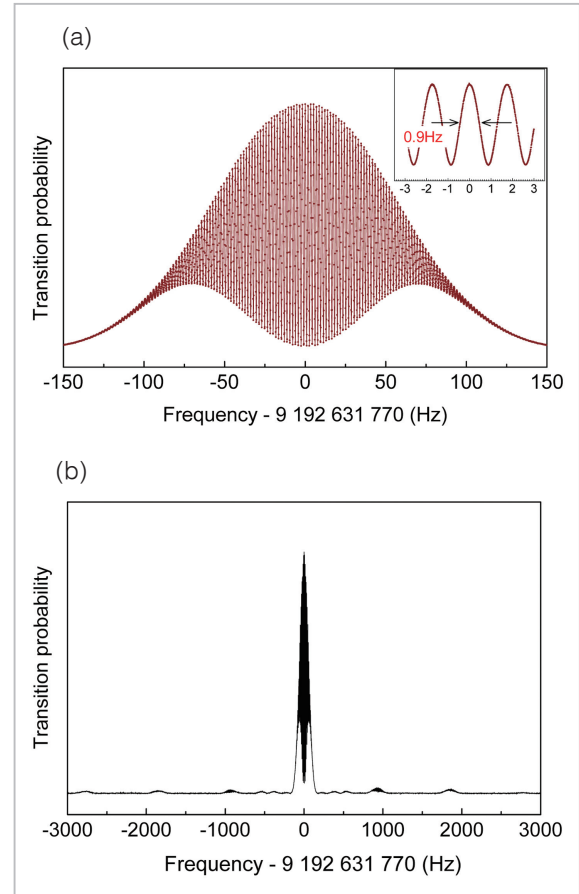


**Fig.3** Ramsey resonance signals in NICT-CsF1

(a) Observed Ramsey fringe pattern of the clock transition in NICT-CsF1. Inset: the enlargement of the central fringes (single-shot data). The atoms are launched up to height of  $38\text{cm}$  above the microwave cavity. The resulting drift time of  $560\text{ms}$  leads to the linewidth of narrower than  $0.9\text{Hz}$ .

(b) Observed Ramsey signals including transitions ( $\pm 900\text{Hz}$ ,  $\pm 1800\text{Hz}$ ,  $\pm 2700\text{Hz}$ ) of  $m_F \neq 0$  components. The total number of all  $m_F \neq 0$  components is  $10\%$  of that of  $m_F = 0$  component. The  $\Delta m_F = \pm 1$  transitions exist at the offset frequency of  $\pm 450\text{Hz}$  with more than  $90\%$  symmetry.

initial velocity of 4.7m/s and the atomic clusters reach a height of 40cm above the microwave cavity. Drift time (the time interval from the 1st interaction to the 2nd interaction)  $T_r$  is 560 milliseconds, and as a result a Ramsey linewidth of 0.9Hz is obtained. The obtained Ramsey signal is shown in Fig. 3(a). Figure 3(b) shows not only  $m_F=0$  component and  $\Delta m_F=0$  transition, but also  $m_F \neq 0$  component  $\Delta m_F=0$  transition and  $m_F=0$  component  $\Delta m_F=\pm 1$  transition.

### 3.2 Frequency stability

In order to precisely determine the central frequency of the obtained Ramsey signal, the microwave frequency is stabilized in the center fringe of the Ramsey signal. Stabilization is carried out via the frequency modulation method. If  $f_0$  is set to the microwave center frequency and  $\Delta\nu$  is set to the Ramsey signal line width, the signal can be observed at frequency  $f_0 - \Delta\nu/2$  and  $f_0 + \Delta\nu/2$  which are the points at which the Ramsey signal slope is greatest. The correction signal sent to the central frequency (to go from  $f_0$  to  $f_1$ ) is proportional to the signal strength difference between the two offset frequencies. The gain of the feedback is chosen such that the transition probabilities at both offsets become equal. The central frequency is then set to this new value ( $f_1$ ) and the Ramsey signal at either offset  $f_1 \pm \Delta\nu/2$  is once again acquired to obtain  $f_2$ . Frequency stabilization is carried out in this manner and the values of the center of the Ramsey signal,  $f_0, f_1, f_2, \dots$ , are recorded. The average of these values is the center frequency of the Ramsey signal.

Figure 4 shows the frequency stability of the Ramsey signal center frequency. The obtained stability is dominated by white frequency noise, indicated by the characteristic slope of  $1/\tau^{1/2}$ . The current frequency stability is  $4 \times 10^{-13}/\tau^{1/2}$ , and the stability is limited by the short-term stability of the hydrogen maser used as a local oscillator and the Dick effect [17].

The slope deviates from  $1/\tau^{1/2}$  at 20,000 seconds and above, due to the long-term drift of hydrogen maser used as a reference. This long-term drift makes evaluation of systematic shifts

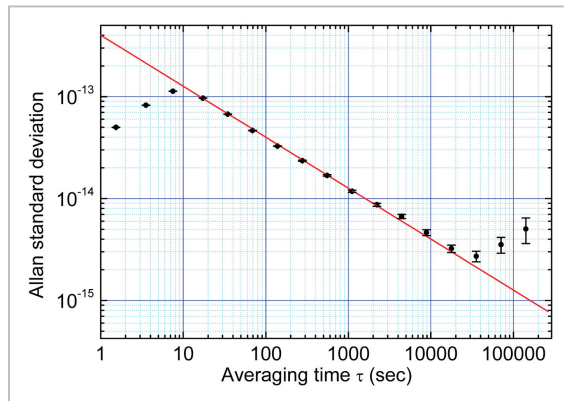


**Fig.4** Allan deviation of the frequency difference between NICT-CsF1 and the hydrogen maser

The short-term stability of  $4 \times 10^{-13}/\tau^{1/2}$  is limited by the phase noise of the LO and the Dick effect.

difficult. In order to eliminate the effect of local oscillator drift, frequency stabilization is carried out under two operating conditions where the parameter of interest is switched between each launch. In this manner two consecutive runs are made where the error signal obtained in each condition feeds back to the center frequency of that condition. This allows drift effects to be eliminated, coming at the cost of an increased cycle time leading to a  $2^{1/2}$  degradation in stability. Nevertheless, it is an effective method for evaluating extremely small shift amounts such as collisional shift and light shift.

## 4 Frequency shifts and their uncertainty

Because extremely narrow line width signals can be observed in atomic fountain standards, the sizes of frequency shifts due to external perturbations are extremely small when compared to thermal beams. As a result the uncertainty in frequency determination will also be small. NICT-CsF1 systematic frequency shift and its uncertainty are theoretically calculated and determined experimentally, as shown in Table 1.

### 4.1 Secondary Zeeman shift

The secondary Zeeman shift is calculated

from the  $|F=4, m_F=1\rangle \rightarrow |F=3, m_F=1\rangle$  transition frequency which has a linear dependence on the magnetic field. Setting the frequency difference between the  $|F=4, m_F=1\rangle \rightarrow |F=3, m_F=1\rangle$  transition and the clock transition as  $\nu_{1-1}$  and omitting high order terms, then the secondary Zeeman shift can be deduced from the Breit-Rabi formula as shown in the following equations[18].

$$\Delta\nu_{2ndZeeman} = \frac{(g_e - g_I)^2 \mu_B^2 \langle B^2 \rangle}{2\nu_0} \quad (4)$$

$$\nu_{1-1} = \frac{(g_e - g_I)}{4} \mu_B \langle B \rangle \quad (5)$$

$$\langle B \rangle = \frac{1}{T} \int_0^T B \cdot dt \quad (6)$$

$g_e$  and  $g_I$  are the  $g$  factors of electron and nucleus,  $\mu_B$  is the Bohr magneton (14 GHz/Tesla),  $\nu_0$  is the clock transition frequency, and  $\langle \rangle$  are the time averages in interaction time  $T$ . If the C-field is uneven,  $\langle B^2 \rangle$  will be expressed as follows.

$$\langle B^2 \rangle = \langle B \rangle^2 + \sigma^2 \quad (7)$$

$\sigma^2$  is the dispersion value of magnetic field  $B$  on the atomic trajectory. Secondary Zeeman shift is expressed in the following equation resulting from equations (4)–(7).

$$\frac{\Delta\nu_{2ndZeeman}}{\nu_0} = 8 \cdot \left( \frac{\nu_{1-1}}{\nu_0} \right)^2 + 427.45 \times 10^8 \cdot \frac{\sigma^2}{\nu_0} \text{ Tesla}^2 / \text{Hz} \quad (8)$$

In order to measure the inhomogeneity of the C-field the frequency of the  $|F=4, m_F=1\rangle \rightarrow |F=3, m_F=1\rangle$  transition was measured at a range of launch heights. The launch height was divided in 7mm steps, and for each different launch height the center frequency was measured. To ensure continuity, those fringes frequencies on either side of the center frequency were also measured. Results are shown in Fig. 5(a).  $\nu_{1-1}$  at actual operation height was 875.1Hz and dispersion  $\sigma$  was 0.4nT. From this the secondary Zeeman shift is determined to be  $72.5 \times 10^{-15}$ , and the shift amount resulting from inhomogeneity was in the  $10^{-19}$  range and can be neglected. In NICT-CsF1, secondary Zeeman shift uncertainty is determined by the  $\langle B \rangle$  time variation.

$$\delta \left( \frac{\Delta\nu_{2ndZeeman}}{\nu_0} \right) = \delta \left[ 8 \cdot \left( \frac{\nu_{1-1}}{\nu_0} \right)^2 \right] = 16 \cdot \frac{\nu_{1-1}}{\nu_0^2} \cdot \delta(\nu_{1-1}) \quad (9)$$

$\delta(\nu_{1-1})$  is the  $\nu_{1-1}$  time variation. It can be deduced from Fig. 5(b) that the  $|F=4, m_F=1\rangle \rightarrow |F=3, m_F=1\rangle$  transition center frequency variation over time is less than 0.5Hz and the secondary Zeeman shift uncertainty is therefore less than  $1 \times 10^{-16}$ .

## 4.2 Collision shift

When caesium atoms are cooled to the microkelvin range, their de Broglie wavelength becomes larger, thus increasing the collisional cross-section. In the operation of the atomic fountain this collisional cross-section is comparatively large and the resulting frequency shift is significantly large. Owing to the difficulty in precisely determining the actual number of atoms the collisional shift uncertainty is

**Table 1** Systematic frequency biases and their uncertainty budgets of NICT-CsF1

| Physical Effect            | Bias  | Uncertainty |
|----------------------------|-------|-------------|
| Secondary Zeeman           | 72.5  | <0.1        |
| Collision*                 | -3.0  | 0.6         |
| Blackbody radiation        | -16.9 | 0.4         |
| Gravitational potential    | 8.4   | 0.1         |
| Microwave power dependence | -0.7  | 0.3         |
| Cavity pulling             | 0.0   | <0.1        |
| Rabi pulling               | 0.0   | <0.1        |
| Ramsey pulling             | 0.0   | <0.1        |
| Spectral impurities        | 0.0   | <0.1        |
| Light shift                | 0.0   | <0.1        |
| Cavity phase               | 0.0   | 0.3         |
| Majorana transition        | 0.0   | <0.1        |
| Background gas             | 0.0   | 0.3         |
| Total (Type B)             |       | 0.9         |

Units are fractional frequency in  $10^{-15}$

\*Typical value

the largest source of uncertainty in the atomic fountain standard. This collisional shift is expressed as [19].

$$\frac{\Delta v_{col}}{v_0} = \frac{nv\lambda(v)}{v_0} \quad (10)$$

where  $n$  is the atomic density,  $v$  is the relative velocity between atoms and  $\lambda$  is the collisional

cross-section area. It is difficult to determine values for each of the parameters in Equation (10), so instead the fountain is operated at a range of  $n$  (the number of atoms) while maintaining the atomic cluster velocity distribution. Extrapolation to  $n=0$  then yields an estimate of the collisional shift. For confident extrapolation, the linearity of the shift as a function of  $n$  (Equation (10)) must be confirmed. Variation of the number of launched atoms is done by changing the strength of the selection cavity microwave signal, thus changing the number excited to the  $|F=3, m_F=0\rangle$  state. Figure 6 shows the time of flight (TOF) signals when atomic density differs. This shows that the TOF signal form and linewidth are exactly the same, and that the number of atoms can be controlled without any changes to relative velocity or collisional cross-section area.

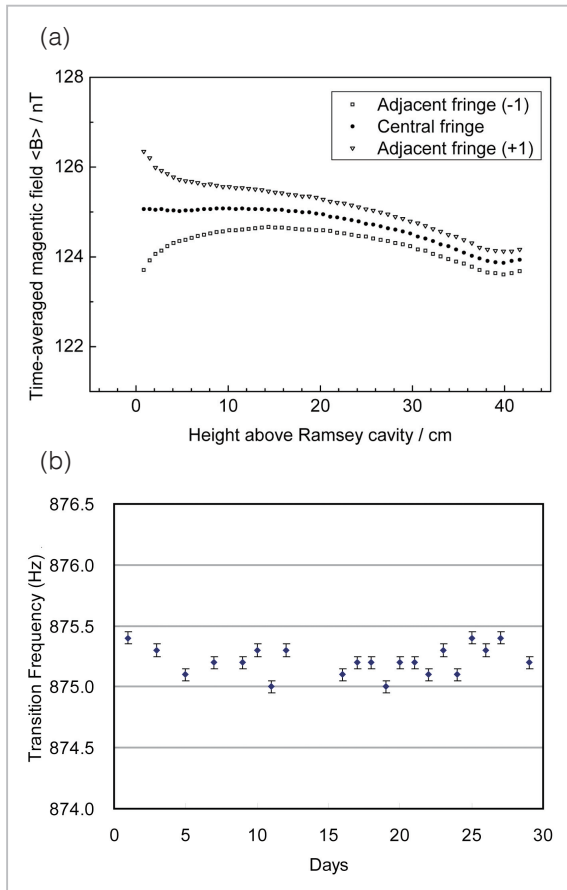


**Fig.5** Magnetic field mapping and time variation of the field

(a) Map of the time-averaged magnetic field over the atomic path with different launching heights. The magnetic intensities are calculated from the central frequency of the  $(F=4, m_F=1) - (F=3, m_F=1)$  transition. The neighboring fringes adjacent to the central one are also measured to avoid misidentification of the central one. At the normal operation, the atoms are launched up to a height of 39.9cm. (b) Tracking of the central frequency of the  $(F=4, m_F=1) - (F=3, m_F=1)$  transition. The temporal variation is less than 0.5Hz, corresponds to 70pT magnetic field variation.

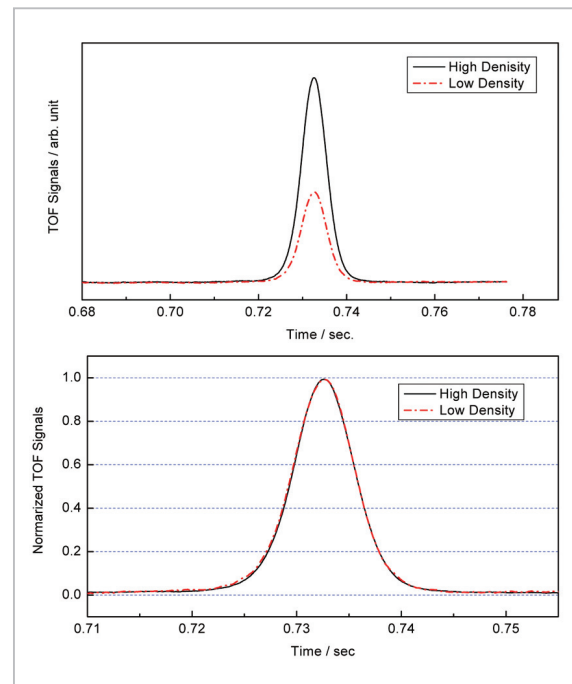


**Fig.6** Observed time-of-flight signals on the way down

The number of atoms, which fly into the Ramsey cavity, is controlled by changing the microwave power in the selection cavity (top graph). Bottom graph show the normalized TOF signals. The line shapes of TOF signals at different densities are almost identical, indicating that the atomic cloud size is practically independent of the atomic number density control.

If each long-term measurement at differing launch number is carried out successively, it will be subject to effects of long-term drifts in the reference signal. To overcome this, two (or more) measurements are interleaved, and any long-term reference signal drifts will be common to both measurements. Figure 7 shows a plot of frequency values when the atomic number density is changed. These are results from over 20 days of observations while changing the atomic number density size. The linearity expressed in Equation (10) can be seen from the obtained results. In addition, by repeating measurements using two different atomic number densities, the linearity is found to be  $\alpha = -8.2$  (standard deviation 1.7). From these results a shift of 20% was assigned for the collision shift uncertainty.

In actual frequency standard operational runs it is only the knowledge of the linearity that is used, not the actual past values. Periodically through the measurement run two atomic number densities are tested in order for extrapolation to  $n=0$ . The typical collision shift value in NICT-CsF1 is  $-3 \times 10^{-15}$  and having an uncertainty of 20% ( $0.6 \times 10^{-15}$ ).

### 4.3 Black body radiation shift

The temperature of the microwave cavity and interaction area is not controlled in NICT-

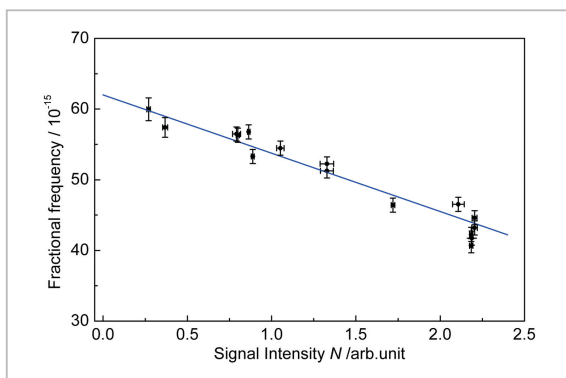


**Fig.7** The fractional frequency difference between NICT-CsF1 and the hydrogen maser as a function of the number of detected atoms.

X-axis indicates the atomic number density in an arbitrary unit, relative to the signal intensity ( $N = 1$ ) at regular operation.

CsF1. To prevent the creation of a new magnetic field by a temperature-control current. As noted above, the room housing NICT-CsF1 is maintained at a very stable temperature of  $25^\circ\text{C}$  ( $\pm 0.2^\circ\text{C}$ ). The frequency shift resulting from black body radiation is expressed in the following equation[4][20].

$$\frac{\Delta v_{BBR}}{v_0} = -1.711 \times 10^{-14} \left( \frac{T}{300} \right)^4 \times \left[ 1 + 0.014 \left( \frac{T}{300} \right)^2 \right] \quad (11)$$

The shift amount at a temperature of 273K is  $-16.9 \times 10^{-15}$  as a result of black body radiation. Taking into consideration the thermal gradient, the temperature uncertainty was set to  $\pm 2\text{K}$  ( $0.4 \times 10^{-15}$ ).

### 4.4 Gravitational red shift

The value of a frequency standard will shift due to gravitational potential (red shift) and thus the SI value is defined as that at the geoid surface (mean sea level). The magnitude of the gravitational red shift can be determined using the following equation[21].

$$\frac{\Delta v_{gravi}}{v_0} = \frac{gh}{c^2} \quad (12)$$

In the atomic fountain the atoms are moving vertically, and thus gravitational red shift will vary over the flight duration. The time-averaged gravitational red shift of atoms moving above the Ramsey cavity is expressed as.

$$\overline{\frac{\Delta v_{gravi}}{v_0}} = \frac{gh_0}{c^2} + \frac{V_0^2}{3c^2} \quad (13)$$

where  $h_0$  is the height from the geoid surface to the Ramsey cavity and  $V_0$  is the atomic velocity when atoms pass through the Ramsey cavity (2.9m/s in NICT-CsF1). For this experiment the evaluation of the height of the Ramsey cavity above the geoid surface was consigned to an external contractor[22]. That height is 114.7 in the GRS80 reference frame, which is equivalent to a height of 76.6m from the geoid surface. The ‘‘GSIGEO2000’’ geoid model was used in the calculation of the geoid

surface[23][24]. The frequency shift amount resulting from the gravitational potential found from this was  $8.4 \times 10^{-15}$ . This measurement has several cm of uncertainty, and the tidal changes caused by the sun and moon cause additional changes in the geoid surface, resulting in an uncertainty in this frequency shift of  $1 \times 10^{-16}$ .

#### 4.5 Microwave power dependent shift

The frequency shift due to the microwave signal in the Ramsey cavity is somewhat complicated, as it is dependent on microwave purity, microwave leakage and cavity structure, which occur in overlapping patterns. Distinguishing these individually is difficult, so instead the microwave power dependence is observed and all related shifts are evaluated collectively. Specifically,  $b\tau$  from Equation (1) is increased by an odd multiple of  $\pi/2$  to observe the frequency variation in NICT-CsF1. Microwave power dependence shift consists of the following 2 types of terms[25]-[27].

- a term which is linearly dependent on the microwave power
- an oscillating term which is dependent on the microwave amplitude (alternating in value between  $\pi/2, 5\pi/2, 9\pi/2 \dots$  and  $3\pi/2, 7\pi/2, 11\pi/2 \dots$ )

By evaluating the dependence which is a composition of these two terms, the frequency shift and uncertainty at normal operation strength ( $b\tau=\pi/2$ ) are found. The results of the microwave power dependence in NICT-CsF1 are shown in Fig. 8. The two terms were fitted by the least square and the shift at normal operating strength was found to be  $-0.7 \times 10^{-15}$ . The uncertainty obtained from the fitting error was  $0.2 \times 10^{-15}$ , however, taking into consideration the lack of measurement points and the fitting flexibility it was set to  $0.3 \times 10^{-15}$ .

#### 4.6 Other shift factors

In addition to the shifts explained previously, it is also necessary to evaluate a variety of other shifts including cavity pulling shift, Rabi and Ramsey pulling shift, shift resulting from Majorana transitions, shift resulting from spectral impurities, background gas shift, light

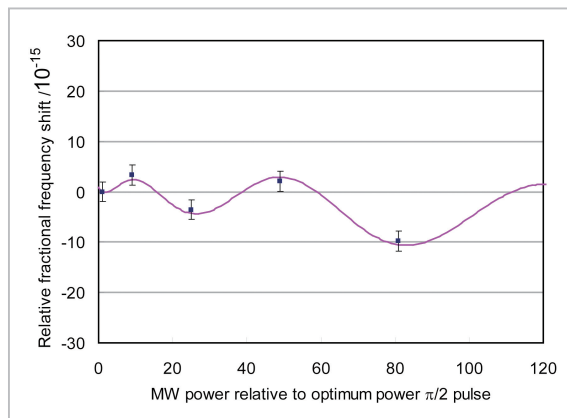


**Fig.8** Measurement of the frequency shift related to the microwave as a function of the microwave power fed to the Ramsey cavity

The data were obtained by the accumulation of a cyclic measurement of  $\pi/2, 3\pi/2, 5\pi/2, 7\pi/2,$  and  $9\pi/2$ , to be free from the instability of the hydrogen maser. By the least square fitting of two contributions [see Section 4.5], the value at zero-microwave field was extrapolated. We evaluated the frequency shift at the optimum power  $(\pi/2)^2$  to be  $-0.7 \times 10^{-15}$  with an uncertainty of  $0.3 \times 10^{-15}$ .

shift and distributed cavity phase shift. If the equipment is built properly, these shifts are small enough that they can be ignored and we treat them as uncertainties (ie. worst case) in determining the total noise budget. See reference [14] for details.

### 5 NICT-CsF1 operation and TAI calibration

NICT-CsF1 is periodically employed in the calibration of the International Atomic Time (TAI) and the Japan Standard Time (UTC (NICT)). Actual NICT-CsF1 operation is carried out as follows. Because TAI values are only calculated every 5 days, accuracy evaluation is commenced on the MJD day of evaluation ending in a 4 or a 9 and then ends on a day ending in a 4 or a 9. For this reason the accuracy evaluation period is the number of days that is a multiple of 5 days (typically 15 days or 20 days). The measurement of the microwave signal stabilized to the central Ramsey signal is carried out and after this accuracy evaluation period systematic shifts that occurred during

operation are determined. Specifically, in order to measure the collision shift amount, NICT-CsF1 is operated before the accuracy evaluation with high and low density launch numbers, and then after measurement the collisional shift correction is applied as described previously. In addition, the external magnetic field is monitored to ensure it does not fluctuate significantly during measurement. To do this, once a day we operate for a short time using the  $|F=4, m_F=1\rangle \rightarrow |F=3, m_F=1\rangle$  transition which is strongly affected by the magnetic field. The value of the magnetic field fluctuation is then used when finding the secondary Zeeman shift. During the measurement period entry to the experiment room is avoided as much as possible to prevent changes in the room temperature and magnetic field environment.

The values are analyzed after the end of the accuracy evaluation period. Firstly the values of the frequency difference between NICT-CsF1 and the reference signal obtained during the accuracy evaluation period are averaged. At present, a hydrogen maser is used as a reference. All frequency shifts are determined and appropriately summed into the final measurement. Additionally, the frequency difference between the reference hydrogen maser and Japan Standard Time is measured using time interval counters and dual mixing time difference (DMTD) measuring equipment, which can then be used to determine NICT-CsF1 frequency value when compared to Japan Standard Time. This value is reported to the BIPM.

$$(f_{CsF1} - f_{HM}) + (f_{HM} - f_{UTC(NICT)}) = f_{CsF1} - f_{UTC(NICT)} \quad (14)$$

At the BIPM, the UTC (NICT) and TAI frequency difference is calculated, finally providing the frequency difference between NICT-CsF1 and TAI.

$$(f_{CsF1} - f_{UTC(NICT)}) + (f_{UTC(NICT)} - f_{TAI}) = f_{CsF1} - f_{TAI} \quad (15)$$

A time scale exists that collects frequency data from a few hundred commercial atomic clocks throughout the world. This is called the Free Atomic Scale (EAL). Although each commer-

cial clock is in itself comparatively noisy, the large ensemble provides a very stable signal. However, despite this high stability the EAL is offset from the definition of a second (TAI) which is determined by, among others, NICT-CsF1. This frequency offset is approximately  $6 \times 10^{-13}$ . The EAL is steered periodically (once per month) to the definition of the SI second using data of primary frequency standards, resulting in the TAI.

The uncertainty of NICT-CsF1 is expressed as the sum of squares of each of the following three types (systematic uncertainty, statistical uncertainty and link uncertainty). The systematic uncertainty, referred to as Type B, is dependent on the experimental setup and is expressed as the sum of squares of all the uncertainties described earlier in this text. Statistical uncertainty is referred to as Type A and is caused by variation in the measurement. For this reason, if the measurement time is increased, the variation is averaged and this value is decreased. In NICT-CsF1, the flicker noise floor reaches  $1.0 \times 10^{-15}$ . It does not progress beyond this level however, due to drifts in the reference signal. Consequentially, the statistical uncertainty is at worst  $1.0 \times 10^{-15}$ . Link uncertainty is composed of the uncertainty of internal links and the uncertainty of time transfer using satellites.

At the 2006 Consultative Committee for Time and Frequency (CCTF) meeting under the Comité International des Poids et Mesures, three requirements were introduced for participation in calibration of the International Atomic Time: confirmation of long-term stability, contribution to comprehensive accuracy evaluation reports and evaluation of the first report submitted to the Bureau International des Poids et Mesures (BIPM) by the Working Group on Primary Frequency Standards. Up until 2006, these were at the discretion of each individual standards institute, but the newly instigated rules ensured the quality of the primary frequency standards. NICT-CsF1 underwent these reviews in 2007, and received international approval as a primary frequency standard able to contribute to the calibration of

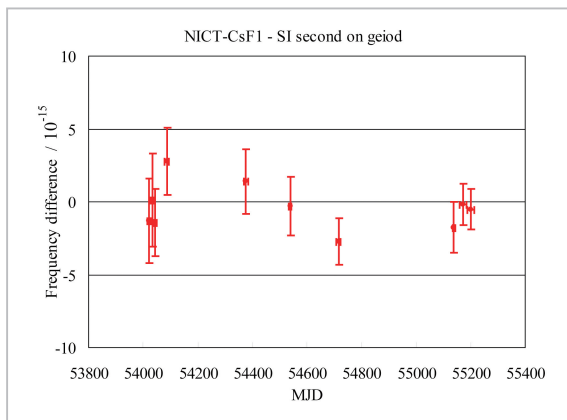


**Fig.9** Frequency difference between NICT-CsF1 and TAI during several campaigns.

X-bar and Y-bar indicates the campaign period and the total uncertainty, respectively. Solid lines and dotted lines show the frequency differences between primary frequency standard and TAI, and uncertainty ranges, respectively, published in *Circular T*.

TAI. Thereafter, at a rate of several times a year, accuracy evaluations have been carried out using NICT-CsF1 and reports of the evaluations sent to the BIPM to contribute to TAI. The results of the accuracy evaluations over several years are shown in Fig. 9. The horizontal error bar represents the measurement period and the vertical error bar represents the total uncertainty including the link uncertainty. The uncertainty has decreased over time due to re-evaluation of frequency shifts and is presently  $1.4 \times 10^{-15}$ .

## 6 Conclusion and future plans

The Space-Time Standards Group has developed the caesium primary frequency standard NICT-CsF1 to contribute to increasing the precision of TAI and the Japan Standard Time. The frequency stability is  $4 \times 10^{-13}/\tau^{1/2}$  and the frequency uncertainty is  $1.4 \times 10^{-15}$ . NICT-CsF1 has thus been used to contribute to TAI calibration. We plan to continue to contribute to TAI and Japan Standard Time.

Although recent remarkable developments of optical frequency standards indicate the role of microwave standards (including fountain clocks) in defining the second is coming to an

end, that time is not now; at the 2009 CCTF meeting a proposal to not redefine the second based on optical standards until 2019 was approved (this does not necessarily mean the second will definitely be redefined in 2019). These extra years are to confirm the validity of optical frequency standards, and in the meantime the definition of the second will continue to be realized through the current microwave standards. Therefore it is necessary to further advance atomic fountain primary frequency standards until at least 2019. Consequently, we are working on the advancement of atomic fountain standards aimed at improvements by one order of magnitude.

In order to improve performance we are focusing on 2 issues: improvement of stability and reduction of uncertainty. If the stability is improved, the time for obtaining the same statistical uncertainty will be decreased by the square of that time, allowing for more precise evaluation of frequency shift. Increasing stability also leads to decreasing uncertainty. The frequency stability of the current NICT-CsF1 is limited by the phase noise of the hydrogen maser used as the reference signal and by the Dick effect. If a reference signal with better short-term stability was used in place of the hydrogen maser, it should increase the stability of NICT-CsF1. As such, we have introduced a cryogenic sapphire oscillator (CSO) which has 100 times better short-term stability than the hydrogen maser (see reference [28] for details). When the CSO was used as the reference signal in place of the hydrogen maser, the frequency stability of NICT-CsF1 was improved by 3 times. This means that the frequency stability achieved up until now can be achieved in 1/9<sup>th</sup> of the time.

In addition, we have begun working on the development of the 2<sup>nd</sup> unit (NICT-CsF2) aimed at reducing the collisional shift, which has the largest uncertainty among the shift factors for atomic fountain primary frequency standards. In NICT-CsF1 atoms are captured using a magneto-optical trap (MOT) which uses magnetic gradients, however because the constraint force is strong, the atomic cluster becomes more

dense, increasing collision shift. In the NICT-CsF2, launching of low density atomic cluster will be possible through capture of atoms using only optical molasses and no magnetic gradient, resulting in a decreased collisional shift. In addition, operating NICT-CsF1 and NICT-CsF2 simultaneously as atomic fountain frequency standards will allow for intercomparison using a common reference signal. We believe that because this will not be affected by long-term drift of the reference signal, it will allow for evaluation of frequency shift factors with even greater precision and lead to reduc-

tion of uncertainty. At present we have succeeded in capturing atoms using only optical molasses and plan to perfect the system as a primary frequency standard hereafter.

In summary, at present the atomic fountain standard is the best frequency standard for realizing the definition of the second. We will carry out the verification of the validity of optical frequency standard values and are considering contributing directly to the TA (NICT) for which independent construction approval has been granted to each research organization.

## References

- 1 M. Hosokawa, "Basic Physics in the Atomic Frequency Standards," *Journal of the National Institute of Information and Communications Technology*, Vol. 50, 3-1, 2003.
- 2 A. Clairon, C. Salomon, S. Guellati, and W. D. Phillips, "Ramsey resonance in a Zacharias fountain," *Europhys. Lett.*, Vol. 16, pp. 165–170, 1991.
- 3 C. Vian, P. Rosenbusch, H. Marion, S. Bize, L. Cacciapuoti, S. Zhang, M. Abgrall, D. Chambon, I. Maksimovic, P. Laurent, G. Santarelli, A. Clairon, A. Luiten, M. Tobar, C. Salomon, "BNM-SYRTE Fountains : Recent Results.," *IEEE Trans. Instrum. Meas.*, Vol. 54, pp. 833–836, 2005.
- 4 R. Wynands and S. Weyers, "Atomic fountain clocks," *Metrologia*, Vol. 42, pp. S64–S79, 2005.
- 5 T. P. Heavner, S. R. Jefferts, E. A. Donley, J. H. Shirley, and T. E. Parker, "NIST-F1: recent improvements and accuracy evaluations," *Metrologia*, Vol. 42, pp. 411–422, 2005.
- 6 K. Szymaniec, W. Chalupczak, P. B. Whibberley, S. N. Lea, and D. Henderson, "Evaluation of the primary frequency standard NPL-CsF1," *Metrologia*, Vol. 42, pp. 49–57, 2005.
- 7 T. Kurosu, Y. Fukuyama, Y. Koga, and K. Abe, "Preliminary Evaluation of the Cs Atomic Fountain Frequency Standard at NMIJ/AIST," *IEEE Trans. Instrum. Meas.*, Vol. 53, pp. 466–471, 2004.
- 8 F. Levi, D. Calonico, L. Lorini, and A. Godone, "IEN-CsF1 primary frequency standard at INRIM: accuracy evaluation and TAI calibrations," *Metrologia*, Vol. 43, pp. 545–555, 2006.
- 9 Y. Hanado, K. Imamura, N. Kotake, N. Nakagawa, Y. Shimizu, R. Tabuchi, L. Q. Tung, Y. Takahashi, M. Hosokawa, and T. Morikawa, "The New Generation System of JAPAN Standard Time at NICT," *Proc. 2006 Asia-Pacific Workshop on Time and Frequency*, pp. 69–76, 2006.
- 10 K. Nakagiri, M. Shibuki, H. Okazawa, J. Umezu, Y. Ohta, and H. Saitoh, "STUDIES ON THE ACCURATE EVALUATION OF THE RRL PRIMARY CESIUM BEAM FREQUENCY STANDARD," *IEEE Trans. Instrum. Meas.*, Vol. IM-36, pp. 617–619, 1987.
- 11 A. Hasegawa, K. Fukuda, M. Kajita, H. Ito, M. Kumagai, M. Hosokawa, N. Kotake, and T. Morikawa, "Accuracy Evaluation of Optically Pumped Primary Frequency Standard CRL-01," *Metrologia*, Vol. 41, pp. 257–263, 2004.
- 12 M. Kumagai, H. Ito, M. Kajita, and M. Hosokawa, "NICT's operational atomic fountain NICT-CsF1," *Proc. 2006 Asia-Pacific Workshop on Time and Frequency*, pp. 77–83, 2006.

- 
- 13 M. Kumagai, H. Ito, M. Kajita, and M. Hosokawa, "Recent Results of NICT Caesium Atomic Fountains," 2007 Proc. Euro. Freq. Time Forum, pp. 602–606, 2007.
  - 14 M. Kumagai, H. Ito, M. Kajita, and M. Hosokawa, "Evaluation of caesium atomic fountain NICT-CsF1," Metrologia, Vol. 45, pp. 139–148, 2008.
  - 15 G. Galzerano, F. Bertinetto, and E. Bava, "Characterization of the modulation transfer spectroscopy method by means of He-Ne lasers and 12712 absorption lines at  $\lambda = 612$  nm," Metrologia, Vol. 37, pp. 149–154, 2000.
  - 16 <http://www.spectradynamics.com/>
  - 17 G. J. Dick, "Local oscillator induced instabilities in trapped ion frequency standards," 1987 Proc. Ann. PTI System and Application Meeting, pp. 133–147, 1987.
  - 18 N. F. Ramsey, "Molecular beam (Oxford: Oxford University Press)," 1956.
  - 19 Vanier J and C. Audoin, "The Quantum Physics of Atomic Frequency Standard (Bristol:Hiulger)," p. 800 1989.
  - 20 E. Simon, P. Laurent, and A. Clairon, "Measurement of the Stark shift of the Cs hyperfine splitting in an atomic fountain." Phys. Rev. A, Vol. 57, pp. 436–439, 1998.
  - 21 J. Vanier and C. Audoin, "The Quantum Physics of Atomic Frequency Standard (Bristol:Hiulger)," pp. 785 1989.
  - 22 <http://www.kkc.co.jp/english/>
  - 23 H. Nakagawa, K. Wada, T. Kikkawa, H. Shimo, H. Andou, Y. Kuroishi, Y. Hatanaka, H. Shigematsu, K. Tanaka, and Y. Fukuda, "Development of a New Japanese Geoid Model, "GSIGEO2000," Bulletin of the Geographical Survey Institute, Vol. 49, pp. 1–10, 2003.
  - 24 Y. Kuroishi, H. Ando, and Y. Fukuda, "A new hybrid geoid model for Japan, GSIGEO2000," J. Geod., Vol. 76, pp. 428–426, 2002.
  - 25 S. R. Jefferts, J. H. Shirley, N. Ashby, E. A. Burt, and G. J. Dick, "Power Dependence of Distributed Cavity Phase-Induced Frequency Biases in Atomic Fountain Frequency Standards," IEEE Trans. Ultrason. Ferroel. Freq. Cont., Vol. 12, pp. 2314–2321, 2005.
  - 26 S. Weyers, R. Schröder, and R. Wynands, "Effects of microwave leakage in caesium clocks: theoretical and experimental results," 2006 Proc. Euro. Freq. Time Forum, pp. 173–180, 2006.
  - 27 K. Szymaniec, W. Chalupczak, S. Weyers, and R. Wynands, "Apparent Power-Dependent Frequency Shift Due to Collisions in a Cesium Fountain," IEEE Trans. Ultrason. Ferroel. Freq. Cont., Vol. 54, pp. 1721–1722, 2007.
  - 28 C.R. Locke, M. Kumagai, H. Ito, S. Nagano, J.G. Hartnett, G. Santarelli, and M. Hosokawa, "Ultra-Stable Cryogenically Cooled Sapphire-Dielectric Resonator Oscillator and Associated Synthesis Chain for Frequency Dissemination," Special issue of this NICT Journal, 2-4, 2010.

(Accepted Oct. 28, 2010)



**KUMAGAI Motohiro, Ph.D.**

*Senior Researcher, Space-Time Standards Group, New Generation Network Research Center*

*Atomic Frequency Standard, Frequency Transfer using Optical Fibers*



**KAJITA Masatoshi, Ph.D.**

*Senior Researcher, Space-Time Standards Group, New Generation Network Research Center*

*Atomic Molecular Physics, Frequency Standard*



**ITO Hiroyuki, Ph.D.**

*Senior Researcher, Space-Time Standards Group, New Generation Network Research Center*

*Atomic Frequency Standard, Optical Frequency Standards*

**HOSOKAWA Mizuhiko, Ph.D.**

*Executive Director, New Generation Network Research Center*

*Atomic Frequency Standards, Space-Time Measurements*